THE JOURNAL OF BIOLOGICAL CHEMISTRY VOL. 291, NO. 30, pp. 15820–15829, July 22, 2016

Regulation of Vacuolar H^+-ATPase (V-ATPase) Reassembly by Glycolysis Flow in 6-Phosphofructo-1-kinase (PFK-1)-deficient Yeast Cells*

Received for publication, January 27, 2016, and in revised form, May 17, 2016 Published, JBC Papers in Press, May 23, 2016, DOI 10.1074/jbc.M116.717488

Chun-Yuan Chan[1], **Dennis Dominguez, and Karlett J. Parra**[2]

From the Department of Biochemistry and Molecular Biology, School of Medicine, University of New Mexico Health Sciences Center, Albuquerque, New Mexico 87131

Yeast 6-phosphofructo-1-kinase (PFK-1) has two subunits, Pfk1p and Pfk2p. Deletion of Pfk2p alters glucose-dependent V-ATPase reassembly and vacuolar acidification (Chan, C. Y., and Parra, K. J. (2014) Yeast phosphofructokinase-1 subunit Pfk2p is necessary for pH homeostasis and glucose-dependent vacuolar ATPase reassembly. *J. Biol. Chem.* 289, 19448–19457). This study capitalized on the mechanisms suppressing vacuolar H^+-ATPase (V-ATPase) in *pfk2*Δ to gain new knowledge of the mechanisms underlying glucose-dependent V-ATPase regulation. Because V-ATPase is fully assembled in *pfk2*Δ, and glycolysis partially suppressed at steady state, we manipulated glycolysis and assessed its direct involvement on V-ATPase function. At steady state, the ratio of proton transport to ATP hydrolysis increased 24% after increasing the glucose concentration from 2% to 4% to enhance the glycolysis flow in *pfk2*Δ. Tighter coupling restored vacuolar pH when glucose was abundant and glycolysis operated below capacity. After readdition of glucose to glucose-deprived cells, glucose-dependent V_1V_o reassembly was proportional to the glycolysis flow. Readdition of 2% glucose to *pfk2*Δ cells, which restored 62% of ethanol concentration, led to equivalent 60% V_1V_o reassembly levels. Steady-state level of assembly (100% reassembly) was reached at 4% glucose when glycolysis reached a threshold in *pfk2*Δ (≥40% the wild-type flow). At 4% glucose, the level of Pfk1p co-immunoprecipitated with V-ATPase decreased 58% in *pfk2*Δ, suggesting that Pfk1p binding to V-ATPase may be inhibitory in the mutant. We concluded that V-ATPase activity at steady state and V-ATPase reassembly after readdition of glucose to glucose-deprived cells are controlled by the glycolysis flow. We propose a new mechanism by which glucose regulates V-ATPase catalytic activity that occurs at steady state without changing V_1V_o assembly.

Vacuolar H^+-ATPase (V-ATPase)[3] is a highly conserved ATP-driven proton pump distributed throughout the endomembrane system. Intracellular V-ATPase generates and maintains the acidic organelle luminal pH necessary for membrane trafficking, protein sorting and processing, and zymogen activation (1–5). V-ATPase is also present at the plasma membrane of cells specialized for active proton transport. Kidney intercalated cells (6), bone osteoclasts (7), and epididymis clear cells (6) express V-ATPases at the plasma membrane, which are necessary for systemic acid-base balance, bone resorption, and sperm maturation, respectively.

V-ATPase consists of two multisubunit domains, V_1 and V_o, that are responsible for ATP hydrolysis and proton transport, respectively (8, 9). Peripheral subunits form V_1, the catalytic domain attached to the cytosolic side of the membrane. V_1 is bound to V_o, the integral membrane domain that forms the path for proton transport. During catalysis, ATP hydrolysis within V_1 drives active transport of protons from the cytosol to the other side of the membrane via rotation of a proteolipid ring structure in V_o. Detachment of V_1 from V_o is an important mechanism that inhibits V-ATPase proton transport (3, 10, 11). Disassembly and reassembly of V_1V_o has been observed in yeast, insects, and mammalian cells (3, 11–13). However, the cellular mechanisms governing V-ATPase regulation by reversible disassembly are not well understood. In yeast, V-ATPase reversible disassembly is intertwined with cytosol pH changes (14, 15) the RAS/cAMP/PKA pathway (16), and glycolysis (3).

Disassembly of the yeast V_1V_o complex occurs when glucose is not available. Upon glucose depletion, V_1 subunit C is released into the cytoplasm, causing the rest of the V_1 domain to dissociate from V_o (10, 17, 18). Disassembly completely inactivates V-ATPase pumps because V_1 without V_o cannot hydrolyze ATP, and V_o without V_1 cannot transport protons (2). Consequently, protons cannot not be redistributed from the cytosol into the vacuole, which alkalinizes the vacuolar lumen and acidifies the cytosol (19, 20). Disassembly is reversed by readdition of glucose to yeast cells (10, 21). After reassembly, V_1V_o resumes ATP-driven proton transport, which restores vacuolar and cytosol pH homeostasis (20).

Complete glucose depletion causes about 75% of the V_1V_o complexes to disassemble (10, 21); the remaining 25% of the pumps maintain the V-ATPase activity necessary to sustain basal cellular functions. Presumably yeast V_1V_o disassembly preserves energy when glucose, the main energy source, is lim-

* This work was supported by National Institutes of Health Grant R01GM086495 (to K. J. P.) and American Heart Association Grant 14PRE19020015 (to C. Y. C.). The authors declare that they have no conflicts of interest with the contents of this article. The content is solely the responsibility of the authors and does not necessarily represent the official views of the National Institutes of Health.

[1] Present address: Van Andel Institute, Grand Rapids, MI 49503.

[2] To whom correspondence should be addressed: Dept. of Biochemistry and Molecular Biology, School of Medicine, University of New Mexico, MSC08 4670, Albuquerque, NM 87131. Tel.: 505-272-1633; Fax: 505-272-6587; E-mail: kjparra@salud.unm.edu.

[3] The abbreviations used are: V-ATPase, vacuolar proton-translocating ATPase; PFK-1, 6-phosphofructo-1-kinase; BCECF-AM, 2′,7′-bis(2-carboxyethyl)-5(6)-carboxyfluorescein acetoxymethyl ester; YEP, yeast extract, peptone medium; YEPD, yeast extract, peptone, 2% dextrose medium.

ited. This hypothesis is supported indirectly by observations that rapidly fermentable carbon sources like glucose, mannose, and fructose trigger reassembly (21), whereas less efficiently fermentable carbon sources like raffinose and galactose or non-fermentable carbon sources like glycerol and ethanol cannot trigger reassembly (10, 21). These studies indirectly linked the V_1V_o assembly levels with glycolysis. Additional evidence suggesting that reassembly correlates with glycolysis comes from studies using the nonmetabolizable glucose analogue 2-deoxyglucose, which cannot substitute for glucose in triggering reassembly (21), and also from studies using a phosphoglucose isomerase (*pgi1*) glycolytic mutant in which fructose, but not glucose, induces V_1V_o reassembly (21).

The glycolytic enzyme aldolase binds to and stabilizes V_1V_o complexes (22, 23). Other glycolytic enzymes, such as 6-phosphofructo-1-kinase (PFK-1) (24, 25) and glyceraldehyde-3-phosphate dehydrogenase (23), co-immunoprecipitate with V-ATPase, although a direct regulatory role on V-ATPase assembly has not been assigned to these enzymes. PFK-1 may be necessary for human kidney V-ATPase function because V-ATPase mutations that cause distal renal tubular acidosis prevent binding of PFK-1 to V-ATPase (25).

Yeast PFK-1 is a hetero-octameric complex ($\alpha_4\beta_4$) (26) that co-purifies with vacuolar membranes and co-immunoprecipitates with V-ATPase subunits (24). The genes *PFK1* and *PFK2* encode the subunits α (Pfk1p) and β (Pfk2p), respectively (26). Because each subunit has catalytic and regulatory functions, yeast cells can form partially active homomeric complexes upon deletion of one PFK-1 structural gene (27). The PFK-1 single deletion mutants *pfk1*Δ and *pfk2*Δ metabolize glucose (27), although at a more reduced rate than wild-type cells. Glycolysis is more severely reduced in *pfk2*Δ than *pfk1*Δ cells (27), indicating that the subunits do not contribute equally to PFK-1 complex activity. In *pfk2*Δ cells, the concentration of fructose 1,6-biphosphate, the PFK-1 reaction product, is 5- to 7.5-fold lower than what is found in *pfk1*Δ cells. Accordingly, *pfk2*Δ exhibits reduced downstream glycolytic intermediates, glucose consumption, and ethanol production (27–29). The fact that *pfk2*Δ does not have detectable glycolytic oscillations (30) indicates that glycolysis self-regulatory functions are defective in this strain.

V-ATPase function is defective in both PFK-1 deletion mutants, but it is more severely impaired in *pfk2*Δ (24). Glucose-dependent V_1V_o reassembly is normal in *pfk1*Δ, but it is reduced by 40–50% in *pfk2*Δ. In addition, V-ATPase proton transport is partially suppressed at steady state. The cells have alkalinized vacuoles and display pH and calcium growth sensitivity, which is characteristic of yeast cells with partially defective V-ATPase activity. The mechanisms by which V-ATPase is suppressed in *pfk2*Δ cells are elusive. Subunit Pfk1p may regulate V-ATPase through its interaction with V_1V_o in the *pfk2*Δ mutant. In addition, a reduction in PFK-1 function and the glycolysis flow may inhibit V-ATPase in *pfk2*Δ cells.

We have now investigated the interrelation between glycolysis and V-ATPase function to gain new knowledge of the mechanisms underlying glucose-dependent V-ATPase regulation. After readdition of glucose to glucose-deprived cells, V_1V_o reassembly is proportional to the glycolysis flow until *pfk2*Δ reaches a metabolic threshold necessary to complete V_1V_o reassembly. At steady state, V-ATPase also communicates with the glycolysis flow. This communication modulates proton transport to restore pH homeostasis when glucose is abundant in *pfk2*Δ. This is a new mechanism by which glucose regulates V-ATPase. It occurs at steady state and does not involve disassembly/reassembly.

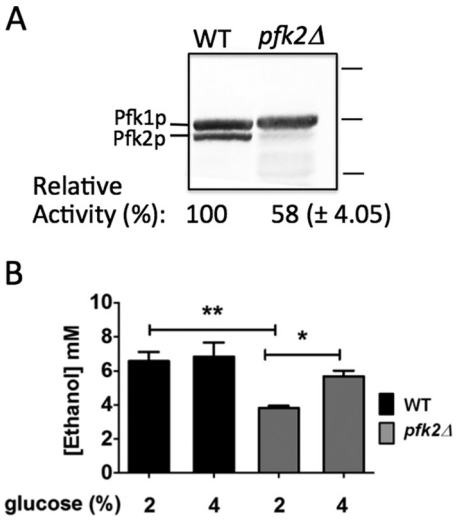

FIGURE 1. **PFK-1 activity and glycolysis are defective in *pfk2*Δ cells**. *A*, PFK-1 enzymatic activity is reduced in *pfk2*Δ cells. Wild-type and *pfk2*Δ cells were grown overnight to mid-log phase (optical density of 0.6–0.8 A_{600}/ml) in YEP medium containing 2% glucose. The cells were converted to spheroplast by zymolase treatment, and protein was separated on a 10% SDS-PAGE gel. The gel was immunoblotted with primary polyclonal antibodies to PFK-1 and secondary antibodies conjugated to alkaline phosphate. Protein markers (*right*) are 150, 100, and 75 kDa. PFK-1 enzymatic activity was measured for an optical density of 20.0 A_{600} obtained from cells grown overnight to mid-log phase in medium containing 2% glucose. Data are expressed as the average ± S.D. ($n = 3$ separate experiments). Relative averaged values were used to express percentage activity. The wild-type PFK-1 activity in the whole cell lysate was 0.014–0.017 μmol of fructose 1,6-bisphosphate/min/optical density A_{600}. *B*, ethanol concentration is lower in *pfk2*Δ than in wild-type cells. The cells were cultured to an optical density of 0.6–0.8 A_{600}/ml in YEP medium containing 2% or 4% glucose, converted to spheroplasts by zymolase treatment, and resuspended in fresh medium containing 1.2 M sorbitol plus 2% or 4% glucose. After 20 min at 30 °C, the ethanol concentration was measured. Data represent three independent experiments. *Error bars* are standard deviation. Statistically significant differences (*, $p < 0.05$; **, $p < 0.01$) were determined by two-tailed unpaired *t* test.

Results

*Stimulation of Glycolysis Rescues V-ATPase Function in pfk2*Δ *at Steady State*—To test the hypothesis that V-ATPase function is adjusted in response to changes in the glycolysis flow, we manipulated glycolysis in *pfk2*Δ cells and measured V-ATPase functions. First, we measured PFK-1 activity in *pfk2*Δ cells to determine the extent of PFK-1 inhibition. As shown in Fig. 1*A*, *pfk2*Δ cells only express subunit Pfk1p. The enzymatic activity of PFK-1 was 42% lower in *pfk2*Δ than wild-type cells. This result is consistent with previous reports indicating that PFK-1 homomeric complexes consisting of subunit α (*pfk2*Δ cells) are less active than wild-type native PFK-1 hetero-octameric complexes ($\alpha_4\beta_4$) (27).

In yeast, the final product of glycolysis, pyruvate, is fermented into ethanol, the levels of which were measured in both strains at steady state (Fig. 1*B*). In the presence of 2% glucose, which is the standard glucose concentration in yeast growth

medium, the ethanol concentration was observed to be 6.6 ± 0.9 mM and 3.8 ± 0.2 mM in the wild-type and *pfk2*Δ strains, respectively. This result indicates that glycolysis was defective in *pfk2*Δ. The 42% ethanol concentration reduction is consistent with the 42% reduction of PFK-1 activity measured in *pfk2*Δ cells and with independent studies that reported reduced fructose-1,6-biphosphate, the 6-phosphofructo-1-kinase reaction product (27–29).

Previous characterizations of glycolysis (27) and V-ATPase pumps (24) in *pfk2*Δ cells were conducted in 2% glucose. Although 2% glucose is optimal for wild-type cells, it might not be optimal for PFK-1 mutants. We reasoned that the *pfk2*Δ glycolytic mutant would require larger concentrations of glucose to maintain a substantial glycolytic flow. The *pfk2*Δ cells were grown in medium containing 2% or 4% glucose, and the ethanol concentration was compared with wild-type cells (Fig. 1*B*). Although lower ethanol levels were detected in 2% glucose, the ethanol concentration increased in 4% glucose in *pfk2*Δ cells. It reached 83% of the ethanol concentration in the wild-type cells, indicating that glycolysis was stimulated.

Because the vacuolar pH is regulated by V-ATPase, vacuolar alkalization is a direct consequence of inhibiting V-ATPase activity. The effects of stimulating glycolysis on V-ATPase proton transport were determined by measuring the vacuolar pH *in vivo*. We used the pH-sensitive fluorophore BCECF, which accumulates in yeast vacuoles. The cells were loaded with BCECF-AM, and the pH was measured fluorometrically according to standard calibration curves (20, 24, 31). The vacuolar pH was measured in wild-type cells and *pfk2*Δ after growing the cells in 2% *versus* 4% glucose. *vma3*Δ cells were used as a control because *vma3*Δ completely lacks V-ATPase function (32). In wild-type cells, where the V-ATPase pumps are fully active, the vacuolar lumen was acidic (pH = 5.2–5.9) at both glucose concentrations (Fig. 2*A*). In 2% glucose, the *pfk2*Δ vacuoles were alkalinized (pH 6.6), similar to the inactive V-ATPase mutant *vma3*Δ (pH 6.8).

In 4% glucose, the acidic pH of the vacuoles was rescued. The *pfk2*Δ vacuolar lumen pH in 4% glucose (pH 5.8) was almost identical to the wild-type vacuolar lumen pH in 2% glucose (pH 5.9). These results show that stimulation of glycolysis with 4% glucose stimulated V-ATPase proton transport in *pfk2*Δ cells at steady state. Thus, they indicate that V-ATPase proton transport is coupled to the flow of glycolysis at steady state.

Sensitivity to elevated pH and calcium at all temperatures is a signature of mutants that lack all V-ATPase activity (vacuolar and Golgi V-ATPase). It is known as the *Vma*$^-$ (vacuolar membrane ATPase) growth phenotype (33) and is only shown when over ~70% of V-ATPase function is compromised (34–36). The *vma* mutants grow at pH 5.0, but growth is reduced or abolished at neutral pH in the presence of high concentrations of calcium (32). The physiological basis of *Vma*$^-$ growth is not fully understood because the downstream consequences of inhibiting V-ATPase are extensive (33). Vacuolar alkalization alone is not sufficient to cause the *Vma*$^-$ phenotype (37). However, *pfk2*Δ growth was fairly reduced with 2% glucose under non-permissive growth conditions at 37 °C (Fig. 2*B*) (24). This modest growth defect was indicative of defective vacuolar but not Golgi V-ATPase function in *pfk2*Δ (37).

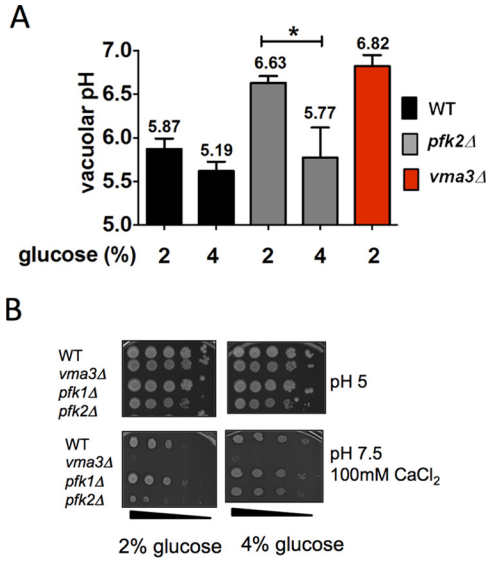

FIGURE 2. **Metabolic reactivation is defective in *pfk2*Δ cells.** *A*, the acidic vacuolar pH is restored in 4% glucose. Wild type, *pfk2*Δ, and *vma3*Δ cells were cultured to mid-log phase in YEP containing 2% or 4% glucose. The cells were harvested and stained with 50 μM BCECF-AM for 30 min at 30 °C. The ratio of fluorescent emission (535 nm) excited at 490 and 450 nm was measured to quantitatively assess vacuolar pH. The average fluorescence over 6 min was compared with a standard curve to generate absolute pH values. Data are presented as average pH values from three independent experiments, and *error bars* are standard deviation. Statistically significant differences (*, $p < 0.05$) were determined by two-tailed unpaired *t* test. *B*, the *vma*$^-$ growth phenotype is rescued in 4% glucose. Cells were cultured to mid-log phase in 2% or 4% glucose, and 10-fold serial dilutions were stamped onto YEP plates containing 2% or 4% glucose adjusted to pH 5.0 and pH 7.5 plus 100 mM $CaCl_2$. Cell growth was monitored for 72 h at 37 °C. Shown are representative plates of triplicates.

To determine whether the *Vma*$^-$ growth is rescued after stimulation of glycolysis, *pfk2*Δ cells were plated on medium containing 100 mM $CaCl_2$ buffered to pH 7.5 (Fig. 2*B*) that was supplemented with 2% glucose (*left panels*) *versus* 4% glucose (*right panels*). The *Vma*$^-$ growth defect was rescued in 4% glucose, indicating that the vacuolar V-ATPase function was restored. As expected, the wild-type strain grew under all the conditions, and *vma3*Δ, which completely lacks V-ATPase function (32), failed to grow under non-permissive conditions. The *pfk1*Δ mutant strain was examined for reference. The *pfk1*Δ strain lacks the PFK-1 subunit Pfk1p but has greater glycolysis flow than the *pfk2*Δ strain (27). The *pfk1*Δ cells closely mimicked the wild-type cells, as reported before (24). A normal *pfk1*Δ growth was consistent with the concept that vacuolar V-ATPase function is coupled to the glycolysis flow.

*Metabolic Reactivation Is Defective in pfk2*Δ *Cells*—Readdition of glucose to cells deprived of glucose rapidly reactivates glycolysis (38–40). We measured ethanol under V-ATPase disassembly (glucose depletion) and reassembly (glucose readdition) conditions to determine whether the glycolysis flow dictates the V-ATPase reassembly level. As described below, glucose-dependent metabolic reactivation was defective in *pfk2*Δ, which cannot sufficiently reassemble V_1V_o after readdition of glucose.

Under disassembly conditions (10 min after glucose removal), the ethanol concentration dropped to about 2.5 ± 0.2 mM in the wild-type and *pfk2*Δ strains (Fig. 3*A*). As a control,

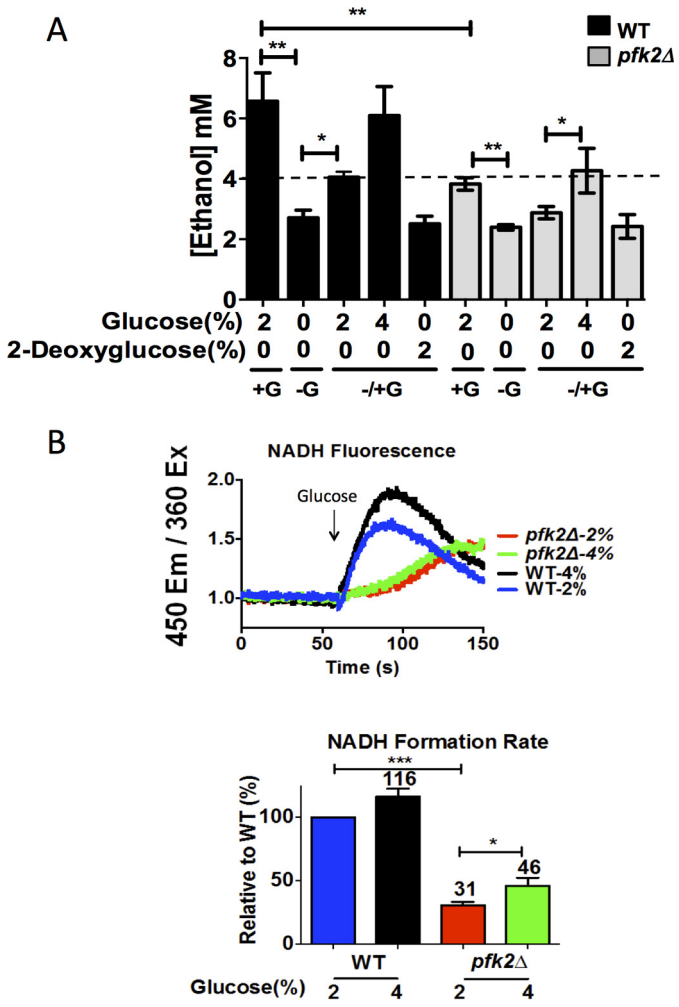

FIGURE 3. **Glucose-induced metabolic reactivation is defective in *pfk2*Δ cells.** *A*, glucose-dependent ethanol formation is decreased in *pfk2*Δ cells. The wild-type and *pfk2*Δ strains were cultured to an optical density of 0.6–0.8 A_{600}/ml in YEP medium containing 2% glucose and converted to spheroplast by zymolase treatment. Spheroplasts were resuspended in fresh medium containing 1.2 M sorbitol and incubated at 30 °C as follows: in the presence of 2% glucose (+ *G*, 20 min), without glucose (− *G*, 10 min), and after readdition of 2% glucose, 4% glucose, or 2% 2-deoxyglucose to glucose-deprived cells (± *G*, 10 min). The ethanol concentration was measured using a colorimetric assay. Data represent three independent experiments. *Error bars* are standard deviation. The *dashed line* represents the ≥40% reassembly threshold. *B*, the rate of NADH formation after glucose re-addition is decreased in *pfk2*Δ cells. Wild-type and *pfk2*Δ cells were cultured overnight in medium containing 2% glucose, and then cells were resuspended in 50 mM potassium phosphate buffer (pH 6.8) for 3 h, after which NADH autofluorescence was monitored (emission (*Em*), 450 nm; excitation (*Ex*) 366 nm) for 60 s in the absence of glucose and for another 120 s after 2% or 4% glucose final concentration was added. Velocities were calculated for the initial 15 s following glucose addition and expressed relative to wild-type cells. Data represent two independent experiments. *Error bars* are standard deviation. Statistically significant differences (*, $p < 0.05$; **, $p < 0.01$; ***, $p < 0.001$) are as compared with the wild type in the presence of 2% glucose and were determined by two-tailed unpaired *t* test.

the ethanol concentration was determined in cells treated with 2-deoxyglucose after glucose was removed. Because of its inability to activate glycolysis beyond 2-deoxyglucose-6-phosphate formation (41), the observed ethanol concentration of 2.5 mM was comparable with that of the glucose-deprived wild type. Because 2-deoxyglucose does not support ethanol production, this indicates that glycolysis had stalled upon removal of glucose.

Under reassembly conditions (10 min after glucose readdition), the concentration of ethanol increased, indicating that glycolysis resumed. Although addition of 2% glucose increased ethanol concentrations to 4.1 ± 0.2 mM and 2.9 ± 0.2 mM in the wild-type and *pfk2*Δ strains, respectively, steady state levels were not reached. These results also showed that 2% glucose resumed glycolysis in the two strains, but to a lesser extent in *pfk2*Δ. The *pfk2*Δ mutant, when 2% glucose was readded, mimicked the wild-type cells deprived of glucose, suggesting that insufficient glycolytic flow upon reactivation is responsible for the V_1V_o reassembly defects in *pfk2*Δ.

Addition of glucose after nutrient limitation is known to trigger a rapid increase of NADH/NAD^+ that inhibits the glycolytic enzyme triose phosphate dehydrogenase (39) and results in a transient peak in NADH levels (42). To monitor the rate of metabolic reactivation when glucose was readded, NADH was measured by autofluorescence. Readdition of 2% glucose stimulated NADH synthesis in wild-type and *pfk2*Δ cells (Fig. 3*B*). However, the NADH synthesis rate was reduced by 70% in *pfk2*Δ cells. These results are consistent with the ethanol measurements, indicating that glucose-mediated metabolic reactivation was defective in *pfk2*Δ.

We measured metabolic reactivation after adding 4% glucose. Fig. 3, *A* and *B*, shows the level of ethanol and NADH formation that resulted from the addition of 4% glucose to *pfk2*Δ after a brief glucose depletion period. The concentration of ethanol reached a steady-state level of 6 mM ± 0.6 mM and 3.8 ± 0.7 mM for the wild type and *pfk2*Δ, respectively. The rate of NADH synthesis in wild-type and *pfk2*Δ cells increased by 15%. It reached up to 46% in *pfk2*Δ cells, which was a larger increase than that observed upon addition of 2% glucose. Thus, doubling the concentration of glucose from 2% to 4% stimulated glucose-dependent metabolic reactivation by about 50% in *pfk2*Δ, as indicated by ethanol levels and the NADH formation rate. Next, we exposed *pfk2*Δ to 2% and 4% glucose to manipulate glycolysis and directly establish the role of glycolysis in V-ATPase assembly and activity.

4% Glucose Rescues Glucose-dependent Reassembly and Vacuolar Acidification—If V_1V_o reassembly is governed by the glycolysis flow, we anticipated reassembly levels to increase after stimulating glycolysis in *pfk2*Δ cells. Fig. 4*A* shows the extent of V_1V_o reassembly in *pfk2*Δ after addition of 4% glucose. Reassembly levels were measured using biosynthetically ^{35}S-radiolabeled cells in pulse-chase experiments as described under "Experimental Procedures." The radiolabeled cells were chased in YEP medium containing 2% glucose for 20 min (steady-state condition, + G), YEP medium without glucose for 10 min (disassembly condition, − G), and after readdition of varied concentrations of glucose (0.1–4%) for an additional 10 min (reassembly conditions, ± G). After the chases, the V-ATPase complexes were immunoprecipitated under nondenaturing conditions with anti-V_1 subunit B to immunoprecipitate V_1 and V_1V_o *versus* anti-V_o subunit a, which can only immunoprecipitate V_o when it is disassembled from V_1.

About 80% of the V_1V_o complexes disassembled upon glucose depletion (Fig. 4*A*). After glucose readdition, reassembly was proportional to the concentration of glucose added. However, *pfk2*Δ required greater concentrations of glucose to reach

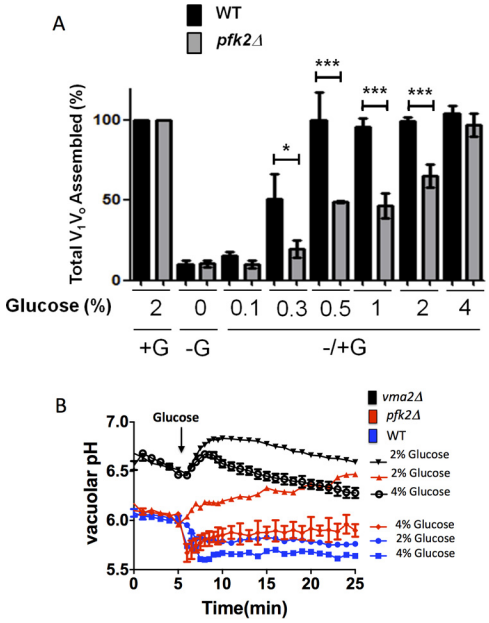

FIGURE 4. **Addition of 4% glucose to glucose-deprived *pfk2*Δ cells rescues V-ATPase reassembly and vacuolar acidification.** *A*, V_1V_o reassembly is glucose-dose dependent. The cells were cultured in 2% glucose, converted to spheroplasts, and biosynthetically radiolabeled with Tran^{35}S. Chases were conducted in the presence of 2% glucose (+ *G*) for 20 min, after glucose depletion (− *G*) for 10 min, and after readdition of varied concentrations of glucose (0.1–4% glucose) (± *G*) for an additional 10 min. The V-ATPase complexes were immunoprecipitated with monoclonal antibodies to V_1 subunit B and V_o subunit a and separated by SDS-PAGE, and then the proportion of total V_o assembled in V_1V_o complexes was estimated. Data were analyzed in a Fuji scanner (FLA-5100) with Multi Gauge and GraphPad Prism 5 software. Results are presented as average from three independent experiments. *Error bars* are standard deviation. Statistically significant differences (*, $p < 0.05$; ***, $p < 0.001$) as compared with steady state (2% glucose) were determined by two-tailed unpaired *t* test. *Error bars* show mean ± S.D. *B*, readdition 4% glucose restores *pfk2*Δ vacuolar acidification after reassembly. Cells were stained with BCECF-AM and deprived of glucose for 10 min in 1 mM HEPE-MES (pH 5.0) buffer, and glucose was readded to a final concentration of 2% or 4% (*arrow*). The ratio of fluorescent emission (535 nm) excited at 490 nm and 450 nm was calculated, and the vacuolar pH was measured using calibration curves. Data represent three independent experiments. *Error bars* are standard deviation.

wild-type levels of reassembly. In the wild-type cells, 50% reassembly was detected after addition of 0.3% glucose; 100% reassembly was reached with 0.5% glucose. In contrast, addition of 0.3% glucose did not trigger significant reassembly in *pfk2*Δ cells, and 2% glucose led to only 60% reassembly. Approaching steady-state levels of assembly (100%) required 4% glucose.

Readdition of 2% glucose, which restored 62% of the steady-state ethanol concentration, triggered comparable levels of V_1V_o reassembly (60%). Readdition of 4% glucose, which restored steady-state ethanol levels led to steady-state reassembly levels (100%). Collectively, these results showed that V_1V_o reassembly was proportional to the glycolysis flow in *pfk2*Δ until the cells reached ≥40% of the steady-state wild-type ethanol concentration and NADH formation rate.

The V_1V_o complexes reactivate after reassembly, which acidifies the vacuolar lumen and restores membrane gradients and secondary transport systems (20). To determine whether reassembly restored V-ATPase proton transport, we measured the vacuolar pH after readdition of 4% glucose to *pfk2*Δ. Vacuolar acidification was detected within 1–2 min of glucose readdition to the wild-type cells (Fig. 4*B*), which is within the timescale when reassembly occurs (3, 21). The V_1V_o reassembly level was somewhat higher in 4% glucose (Fig. 4*A*), and the wild-type vacuole pH was slightly more acidic.

Glucose-induced acidification was defective in *pfk2*Δ in response to 2% glucose even though 60% of the V_1V_o complexes reassembled in the glycolytic mutant (Fig. 4*A*). However, V-ATPase proton transport resumed after 4% glucose readdition. Reactivation of V-ATPase proton transport was indicated by the rapid acidification of the vacuolar lumen. The *vma2*Δ strain that cannot assemble V_1V_o complexes (43) was used as a negative control because *vma2*Δ completely lacks V-ATPase activity and vacuolar buffering capacity (2). As expected, the net vacuole pH was considerably more alkaline in *vma2*Δ than in wild-type and *pfk2*Δ cells. A gradual pH drop was detected in *vma2*Δ at 3 min after V-ATPase reactivation (acidification) was complete in wild-type and *pfk2*Δ cells (Fig. 4*B*). This observation further indicated that glucose-mediated vacuolar acidification was V-ATPase-dependent in *pfk2*Δ cells.

Proton Transport Is Increased at Vacuolar Membranes—The rates of proton transport and ATP hydrolysis were measured in purified vacuolar membranes from *pfk2*Δ cells. V-ATPase activity was determined in the presence and absence of the specific V-ATPase inhibitor concanamycin A, and the ratio of proton pumping to ATP hydrolysis was used as a means of estimating the coupling efficiency of the enzyme when glycolysis was stimulated in *pfk2*Δ cells.

In wild-type cells cultured in 4% glucose, ATP hydrolysis and proton transport activities increased by 21% and 17%, respectively, compared with those grown in 2% glucose (Fig. 5*A*). In contrast, ATP hydrolysis was unchanged in *pfk2*Δ membranes from cells cultured in 2% *versus* 4% glucose, which was 64–67% of the wild-type ATP hydrolysis. However, proton transport significantly increased (by 30%) when *pfk2*Δ cells were grown in 4% glucose from that observed in 2% glucose. As a result, the proton transport/ATP hydrolysis ratio increased 24% in the *pfk2*Δ mutant (from 0.63 to 0.83). Western blotting analyses of vacuolar membrane fractions showed comparable levels of V_1 subunit A and subunit B in 2% glucose and 4% glucose (Fig. 5*B*). Based on these results, we concluded that the V-ATPase pumps fine-tuned their catalytic activity in 4% glucose, which enabled *pfk2*Δ cells to restore vacuolar pH homeostasis.

Pfk1p Subunit Binding to V-ATPase Decreases in 4% Glucose—The individual PFK-1 subunits expressed in *pfk1*Δ (subunit Pfk2p) and *pfk2*Δ (subunit Pfk1p) cells co-immunoprecipitate with V-ATPase and co-purify with vacuolar membrane fractions (24). Thus, deletion of one PFK-1 subunit does not prevent interaction of the other subunit with V-ATPase.

We asked whether binding of the subunit Pfk1p to V-ATPase was affected in 4% glucose in the *pfk2*Δ mutant. The level of Pfk1p subunit co-immunoprecipitated with the anti-V_1 subunit A monoclonal antibodies that recognize V_1 and V_1V_o complexes (21) was analyzed. About 60% fewer Pfk1p co-immunoprecipitated with V_1 subunits in *pfk2*Δ cells in 4% glucose (Fig. 6). This decrease in Pfk1p-V-ATPase binding was not caused by change in expression of Pfk1p and/or V-ATPase subunits because these protein expression levels were comparable in whole cell lysates from 2% and 4% glucose (Fig. 6, *Input*). Rather, Pfk1p-V-ATPase binding was decreased in 4% glucose

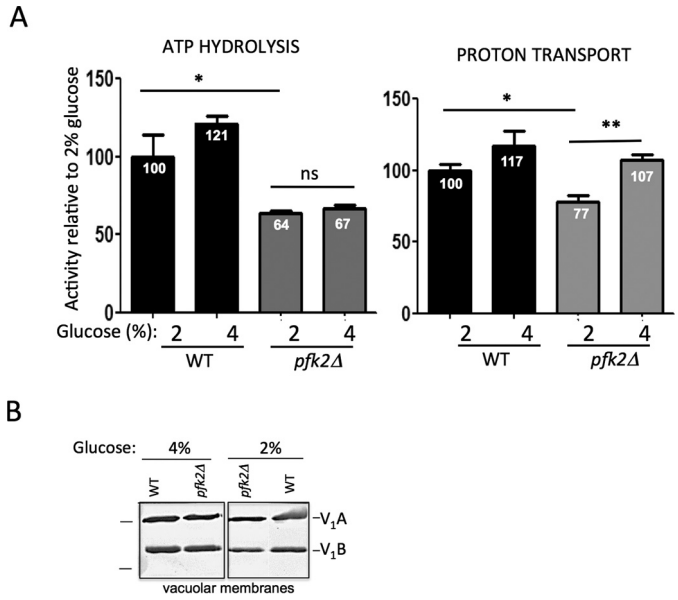

FIGURE 5. **Proton transport is increased at vacuolar membranes from *pfk2*Δ cells cultured in 4% glucose.** *A*, V-ATPase coupling efficiency is increased in 4% glucose. Vacuolar membrane fractions from wild-type and *pfk2*Δ cells were purified by density centrifugation. ATP hydrolysis (*left panel*) was assayed spectrophotometrically in the presence and absence of the V-ATPase inhibitor concanamycin A (100 nM) by using an enzymatic coupled assay that measures NADH oxidation at 340 nm. The average wild-type specific activity in 2% glucose for the concanamycin A-sensitive ATP hydrolysis was 3.0 μmol of ATP/min/mg of total vacuolar protein. ATP-dependent proton transport (*right panel*) was measured by fluorescence quenching of 1 μM 9-amino-6-chloro-2-methoxyacridin (excitation, 410 nm; emission, 490 nm) upon addition of 0.5 mM ATP/1 mM $MgSO_4$ to 5 μg of total protein in vacuolar membrane vesicles. Initial velocities were calculated for 15 s following MgATP addition. The average wild-type slope was −1117.47 fluorescence units/15 s. Data represent six independent vacuolar preps. Statistically significant differences (*, $p < 0.05$; **, $p < 0.01$; *ns*, not significant) were as compared with the wild type in the presence of 2% glucose and determined by two-tailed unpaired *t* test. *B*, V-ATPase assembly is comparable in 4% glucose and 2% glucose. Vacuolar membrane vesicles were purified from *pfk2*Δ and wild-type cells cultured overnight in 2% glucose or 4% glucose. Membrane protein (1 μg total membrane protein/well) was separated by SDS-PAGE in 10% gels. Gels were immunoblotted with primary monoclonal antibodies to V_1 subunit A and subunit B, and secondary antibodies conjugated to alkaline phosphate. Protein markers (*left*) are 77 and 50 kDa. This gel was modified to excise a lane containing *pfk1*Δ membranes.

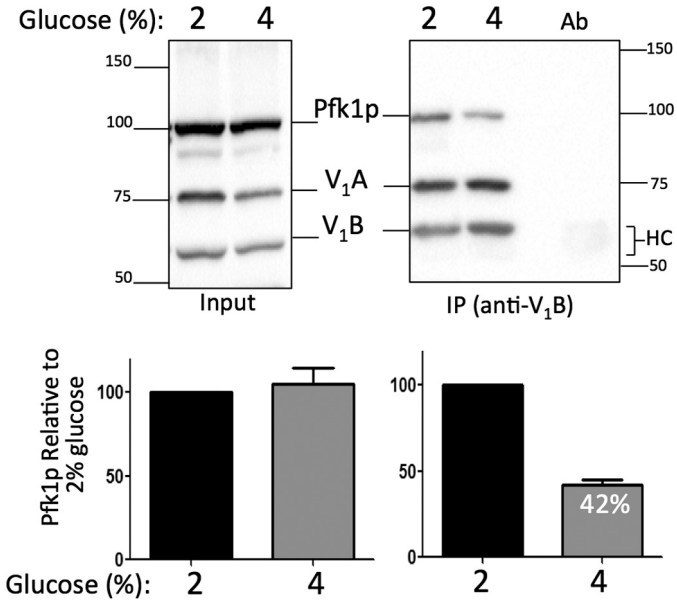

FIGURE 6. **Pfk1p subunit binding to V-ATPase decreases in 4% glucose.** Overnight mid-log phase cultures (optical density of 0.8–1.0 A_{600}/ml) were lysed, and V-ATPase complexes were immunoprecipitated with anti-A monoclonal antibody. Immunoprecipitated protein (*IP*) and total lysate protein (*Input*) were loaded on 10% SDS-PAGE gels. Pfk1p and V-ATPase (V_1 subunits A and B) were detected by immunoblots using, respectively, anti-PFK-1 polyclonal antibodies and anti-B and anti-A monoclonal antibodies and horseradish peroxidase secondary antibodies. *Ab*, antibody alone; *HC*, antibody heavy chain. Protein markers are 150, 100, 75, and 50 kDa. A representative gel is shown (*top panel*). Gels from two independent experiments were scanned using a Bio-Rad ChemiDoc XRS+, and data were analyzed using Multi Gauge V3.0 and GraphPad Prism 5 software. Data were expressed as –fold increase Pfk1p:V_1 subunit ratio ± S.D. relative to the wild type (*bottom panel*).

in *pfk2*Δ, which was suggestive of lower Pfk1p-V-ATPase binding affinity in this mutant.

Discussion

This study capitalized on the cellular mechanisms suppressing V-ATPase function in *pfk2*Δ to gain new knowledge of the mechanisms underlying glucose-dependent V-ATPase regulation. We took advantage of the fact that V-ATPase is fully assembled in *pfk2*Δ cells at steady state and glycolysis partially suppressed to manipulate the glycolysis flow and assess its direct involvement on V-ATPase function.

At steady state, the ratio of proton transport to ATP hydrolysis increases in response to high glucose levels in *pfk2*Δ. Enhanced V-ATPase proton transport restores vacuolar pH homeostasis. It likely allows cells to preserve energy when glycolysis is suboptimal and glucose abundant (4% glucose). One importance of these findings is that they revealed V-ATPase elasticity of coupling as a new mechanism of how glucose regulates V-ATPase pumps without changing the V_1V_o assembly state. This study also showed that, under V_1V_o reassembly conditions, the level of glucose-induced reassembly directly corresponds to the glycolysis flow in *pfk2*Δ cells. V_1V_o reassembly is complete after the rate of glycolysis reaches a threshold (40–46% of the wild-type rate in 2% glucose) when metabolism resumes after glucose is readded to glucose-deprived cells.

The Glycolysis Flow Communicates with V-ATPase and Regulates Its Activity at Steady State—At steady state, in 2% glucose, the ethanol concentration is significantly reduced (by 42%) in *pfk2*Δ cells. This level of glycolytic reduction mimics the level of PFK-1 activity reduction (42%) (Fig. 1*A*), as expected, because PFK-1 catalyzes the second limiting step reaction of the pathway.

V-ATPase proton transport is suppressed in 2% glucose in *pfk2*Δ. Consequently, the vacuolar lumen is alkalinized (Fig. 2*A*). This alteration in V-ATPase function is not due to V_1V_o disassembly or catalytic defects because *pfk2*Δ cells cultured in 2% glucose display wild-type levels of V_1V_o complexes at the membrane and express catalytically competent wild-type V-ATPase pumps (24). Rather, vacuolar V-ATPase function is inhibited *in vivo* in *pfk2*Δ cells cultured in 2% glucose. This study indicates that V-ATPase activity is suppressed in *pfk2*Δ because glycolysis is suppressed. Regulation of V-ATPase activity at steady state by the glycolysis flow has not been reported before.

V-ATPase activity is remarkably sensitive to changes in the glycolysis flow. Addition of 4% glucose restores 83% of wild-type ethanol concentration at steady state (Fig. 1*B*). This signif-

icant stimulation of glycolysis also restores the vacuolar acidic pH (Fig. 2*A*). This result is indicative of a causal correlation between the glycolysis flow and V-ATPase activity. It is evidence that glucose regulates V-ATPase activity at steady state. Accordingly, the PFK-1 subunit deletion mutant *pfk1*Δ, which has milder glycolysis defects than *pfk2*Δ (27), has milder V-ATPase alterations (24). Thus, V-ATPase proton transport is adjusted in response to the glycolytic flow at steady state.

V-ATPase Adjusts Catalytic Activity in Response to Glucose When Glycolysis Is Suboptimal—V-ATPase catalytic coupling is tighter in *pfk2*Δ cells in 4% glucose (Fig. 5*A*) when glycolysis operates below capacity at steady state. The proton transport/ATPase ratio increases by 24%, indicating that V-ATPase is more efficient (transports more protons per ATP hydrolyzed), probably to help cells to preserve energy. Importantly, these findings indicate that ATP hydrolysis and proton transport by V-ATPase pumps may not always be optimally coupled *in vivo*.

Using *pfk2*Δ cells, this study showed that glucose can control V-ATPase activity without changing the V-ATPase assembly state. Until now, glucose-dependent regulation of yeast V-ATPase has been via V_1V_o disassembly and reassembly in response to glucose depletion and readdition, respectively (3). Although the ability of V-ATPase to change coupling of ATP hydrolysis and proton pumping has been described before (44), the involvement of glucose and glycolysis has not been reported. Increased efficiency of coupling was observed in some genetic mutants (45) and when V-ATPase pumps were exposed to low ATP concentrations *in vitro* (46). In yeast, the N-end domain of V_o subunit a (47, 48) and a non-homologous region of the V_1 subunit A (45) have been implicated in this type of regulation.

Changes in the proton transport to ATPase activity ratio may be linked to "loose" conformations required for disassembly and reassembly because, during catalysis, relative rotation of V_1 and V_o subunits requires stable V_1V_o assembly. Accordingly, catalytic slip does not occur in the molecular motors that do not reversibly disassemble, such as the F_1F_o ATP synthase. One possibility is that, in 4% glucose, V_1V_o intermediary structures that slip during catalysis are stabilized in *pfk2*Δ to restore the membrane pH gradients necessary for an array of other transporters when glucose concentration is high (20).

Complete V_1V_o Reassembly after Glucose Readdition Requires the Glycolysis Flow to Reach a Threshold—Glucose depletion, which inhibits glycolysis, leads to V_1 dissociation from V_o, and its readdition, which resumes glycolysis, causes V_1 to reassociate with V_o (3). Thus, yeast V-ATPase assembly is intimately linked to the glycolysis flow.

We reasoned that if a metabolic input drives V_1V_o reassembly, then it would reach a certain threshold within the first minutes after glucose readdition to glucose-deprived cells. Below this threshold, reassembly is defective. We found the threshold to be 40–46% of the wild-type glycolytic capacity. We have chosen to monitor the glycolytic intermediate NADH to establish the metabolic threshold for reassembly after glucose readdition. The NADH formation rate corresponds to the rate of glycolysis. In addition, NADH autofluorescence is measureable in intact cells in real time. The wild-type NADH formation rate in 2% glucose is used as a reference for these studies because 2% is the standard glucose concentration in yeast growth medium.

When 2% glucose is readded, the NADH formation rate is only 31% of the wild-type rate. Under these conditions, the *pfk2*Δ cells cannot sufficiently reassemble V_1V_o. Addition of 4% glucose, which stimulates the rate of glycolysis to 46% (the proposed NADH threshold), prompts wild-type levels of V_1V_o reassembly in *pfk2*Δ (Fig. 4*A*). Likewise, V_1V_o reassembly is complete when the cells produce ≥40% the wild-type ethanol levels (Fig. 3*A*). With reassembly, V_1V_o proton transport resumes, and the vacuoles are acidified after 1–2 min of 4% glucose readdition to *pfk2*Δ.

The finding that V_1V_o remains silenced in *pfk2*Δ after readdition of 2% glucose even though 60% of the V-ATPase complexes are reassembled is intriguing. It can be explained if inhibitory MgADP is trapped in the catalytic sites (49) because glycolysis is significantly suppressed. Alternatively, a regulatory subunit such as V_1 subunit H, which silences V_1 after disassembly (49) and activates V_1V_o complexes at the membrane (50), could have retained an inhibitory conformation preventing proton transport in 2% glucose (51, 52).

Although glycolytic ATP formation is an attractive possibility to signal reassembly and/or reactivation in 4% glucose, the levels of ATP during glucose deprivation and readdition do not appear to correlate to the V-ATPase assembly state (21). Wild-type yeast cells recover steady-state ATP concentrations in the absence of glucose (21).

How Does PFK-1 Regulate V-ATPase Activity?—The finding that V-ATPase function is fully rescued in 4% glucose in *pfk2*Δ cells that lack the *PFK2* gene argues against direct regulation of V-ATPase through its physical interaction with the PFK-1 subunit Pfk2p. However, the PFK-1 subunit Pfk1p may play an inhibitory role in *pfk2*Δ cells. The level of Pfk1p that co-immunoprecipitates with V-ATPase subunits is significantly reduced in *pfk2*Δ cells in 4% glucose (Fig. 6). This decrease can be explained if Pfk1p is recruited to support greater glycolytic demands in 4% glucose, after which V-ATPase proton transport is enhanced. Whether binding of subunit Pfk1p to V-ATPase is inhibitory is an interesting possibility that will be addressed in future studies.

This study showed that at least one mechanism by which PFK-1 modulates V-ATPase is via the glycolysis flow. The RAS/cAMP/PKA signaling pathway, which has been linked to glucose-dependent V_1V_o disassembly and reassembly, is also intertwined with PFK-1. Activation of the RAS/cAMP/PKA pathway enhances the glycolysis flow because PKA stimulates formation of fructose-2,6-bisphosphate, the most potent activator of PFK-1. Thus, RAS/cAMP/PKA could control V-ATPase assembly via glycolysis (16).

We cannot eliminate the possibility that glucose-dependent pH changes could also regulate V-ATPase. Cytosol alkalization is glucose concentration-dependent and correlates to the level of V_1V_o assembly (14, 53). A larger ΔpH between the cytosolic and the luminal sides of the vacuolar membrane may stimulate V_1V_o activity. Similar to the activating effect ΔpH has on the F_o subunit a of the evolutionary related F-ATP synthase (54), binding of protons to the membrane-bound V_o subunit a of the V-ATPase could prime V_1V_o proton transport. In *Arabidopsis*,

the V-ATPase coupling ratios are sensitive to the cytosol and vacuolar pH (55). In the lemon fruit, variable coupling and pH-dependent slip regulate the V-ATPase pump (56).

Clearly, the scope of glucose-dependent V-ATPase regulation is more complex than initially anticipated. It extends beyond V_1V_o disassembly and/or reassembly and is intimately linked to the metabolic state of a cell, specifically the glycolysis flow. The finding that V-ATPase changes catalytic efficiency when the cellular demands for membrane transport increase (4% glucose) and glycolytic ATP production operates below capacity can have implications in human health, particularly for distal renal tubular acidosis (25), viral infections (57), and the metabolic switch in cancers (58, 59), where glucose-dependent regulation of V-ATPase is conserved.

Experimental Procedures

Materials and Strains—The Tran[^{35}S]-label was from MP Biomedicals (Santa Ana, CA). The antibodies anti-Myc, anti-phosphoglycerate kinase 1 (22C5D8), and anti-V-ATPase (10D7 and 13D11) were from Invitrogen. Alkaline phosphatase-conjugated secondary antibodies were from Promega (Madison, WI) and horseradish peroxidase secondary antibodies from Invitrogen. Zymolase 100T was purchased from Seikagaku (Tokyo, Japan), concanamycin A from Wako Biochemicals (Richmond, VA), and Ficoll and carbonyl cyanide *m*-chlorophenylhydrazone from United Stated Biologicals (Swampscott, MA). The ATP assay kit (K354-)100 was purchased from Biovision (Milpitas, CA) and the ethanol assay kit (ab65343) from Abcam (Cambridge, MA). All other reagents were from Sigma. The *Saccharomyces cerevisiae* strains referred to throughout are BY4742 wild-type (*MATα; his3Δ1; leu2 Δ; lys2Δ; ura3Δ*), BY4742 *pfk1* (*pfk1Δ:KanMX6*), BY4742 *pfk2Δ* (*pfk2Δ:KanMX6*), and BY4742 *vma3Δ* (*vm3Δ:KanMX6*). The mutant strains *pfk2Δ* and *pfk1Δ* were verified by PCR using primers to amplify the *PFK2* and *PFK1* genes with 5′-XhoI and 3′-XmaI cutting sites.

Growth Phenotype—Cells were grown overnight to 0.6–1.0 A_{600}/ml in YEPD medium buffered to pH 5.0 with 50 mM succinic acid/50 mM sodium phosphate. Cultures were washed twice with sterile double-distilled H_2O and cells with an optical density of 2.5 A_{600} were resuspended into 1 ml of sterile double-distilled H_2O. 10-fold serial dilutions were stamped onto YEP containing 2% glucose and 4% glucose. Plates were buffered to pH 5.0 with 50 mM succinic acid/50 mM sodium phosphate (pH 7.5) with 50 mM MES/50 mM MOPS or pH 7.5 with 100 mM calcium chloride added. The plates were incubated for 72 h at 30 °C and 37 °C.

Vacuolar pH—Vacuolar pH was measured using the ratiometric fluorescent dye BCECF-AM (31, 60). Cells were grown to an optical density of 0.6–1.0 A_{600}/ml and stained with 50 μM BCECF-AM for 30 min at 30 °C. Calibration curves were generated as described before (20) in calibration buffers (pH 5.5, 5.75, 6.0, 6.25, 6.5, and 7) consisting of 50 mM MES, 50 mM HEPES, 50 mM KCl, 50 mM NaCl, 200 mM ammonium acetate, 10 mM sodium azide, 10 mM 2-deoxyglucose, and 50 μM carbonyl cyanide *m*-chlorophenylhydrazone. For steady-state analyses of the vacuolar pH, the BCECF-stained cells were transferred to 1 mM HEPE/MES (pH 5.0) buffer with 2% or 4% glucose (final concentration), and BCECF fluorescence (ratio of 490/450 nm, 525 nm excitation) was measured for 10 min at 30 °C in a FluoroMax 4 spectrofluorometer (Horiba Jobin Yvon Inc.). Data collected between 3 and 8 min were averaged. For V-ATPase disassembly/reassembly conditions, BCECF-stained cells were deprived of glucose on ice for 10 min, and the vacuolar pH was monitored 20 min after 2% or 4% glucose readdition (final concentration).

Immunoprecipitations—Pulse-chase experiments were conducted at the indicated glucose concentrations and times following protocols described before (21). The V-ATPase complexes were immunoprecipitated from whole cell lysates with the monoclonal antibodies 13D11 (anti-V_1 subunit B) and 10D7 (anti-V_o subunit a, Vph1p isoform) and the protein separated by SDS-PAGE (13% acrylamide gels). The gels were dried, scanned in a Fuji scanner (FLA-5100), and analyzed using Multi Gauge and GraphPad Prism 5 software as described previously (24). The proportion of V_o assembled into V_1V_o, determined by comparing the amount of V_o subunit a immunoprecipitated with 13D11 with the total amount of V_o subunit a immunoprecipitated with both antibodies. For non-radiolabeled immunoprecipitations, the 13D11 antibody was used to immunoprecipitate V-ATPase from whole cell lysates (61). Protein was separated by SDS-PAGE in 10% gels and analyzed by Western blotting using the monoclonal antibodies 8B1 (anti-V_1 subunit A) and 13D77 (anti-V_1 subunit B) and yeast PFK-1 polyclonal antibodies. The nitrocellulose membranes were blotted with horseradish peroxidase secondary antibody and scanned using a Bio-Rad ChemiDoc XRS+, and then the intensity of protein bands was quantified using Multi Gauge and GraphPad Prism 5 software.

NADH Autofluorescence—NADH was monitored as described by Poulsen *et al.* (42) with the following modifications. The cells were grown overnight to an optical density of 0.6–1.0 A_{600}/ml in YEPD, harvested, and cells with an optical density of 100 A_{600} were resuspended in 50 mM potassium phosphate buffer (pH 6.8) up to a density of 10% by weight. The cells were starved of glucose by incubation in the same phosphate buffer for 3 h on a rotary shaker at 30 °C and placed on ice for 10 min. The NADH fluorescence intensity (excitation at 366 nm, emission at 450 nm) was monitored without glucose for 60 s and then continuously recorded for an additional 90 s with readdition of 2% glucose or 4% glucose at 30 °C in a FluoroMax 4 spectrofluorometer (Horiba Jobin Yvon Inc.).

Ethanol Concentration—For steady-state analyses, the cells were cultured overnight to an optical density of 0.6–1.0 A_{600}/ml in YEP (pH 5.0) medium (wild-type and *pfk2Δ*) containing 2% or 4% final glucose concentration. Cells with a total of 2.0 optical density A_{600}/ml per condition were harvested and then converted to spheroplasts by zymolase treatment (35). The spheroplasts were incubated at 30 °C for 10 min in YEP adjusted to pH 5.0 with 50 mM succinic acid/50 mM sodium phosphate containing 2% or 4% glucose plus 1.2 M sorbitol. The ethanol concentration was measured using an ethanol assay kit (ab65343, Abcam) according to the instructions of the manufacturer. For glucose-depletion and readdition analyses, the cells were grown in medium containing 2% glucose overnight and converted to spheroplasts as described above, and then the

spheroplasts were incubated in YEP medium with 2% or 4% glucose for 20 min, in YEP for 10 min, and in YEP for 10 min, followed by addition of 2% glucose, 4% glucose, or 2% 2-deoxyglucose for 10 min.

PFK-1 Enzymatic Activity—Wild-type and *pfk2*Δ cells were cultured overnight to an optical density of 0.6–1.0 A_{600}/ml in YEPD (pH 5.0) medium. Cells were converted to spheroplasts and lysed in 15 mM MES-Tris (pH 6.9) containing 5% glycerol at a final concentration of 1.0 optical density A_{600}/μl. PFK-1 activity was measured spectrophotometrically at 37 °C using the coupled enzyme assay of Lotscher *et al.* (62). Whole cell lysates (20.0 optical density A_{600}) was added to the enzymatic assay mixture (25 mM Tris (pH 6.9), 2 mM ATP, 5 mM $MgCl_2$, 2 mM phosphoenol pyruvate, 30 units/ml pyruvate kinase, 30 units/ml L-lactic dehydrogenase, and 0.5 mM NADH), and the reaction was started by addition of 5 mM fructose-6-phospate. NADH oxidation was monitored spectrophotometrically at 340 nm for 5 min. One unit of PFK-1 activity is defined as 1 μmol fructose 1,6-bisphosphate formed/min in an optical density of 20 A_{600}.

Other Methods—Vacuolar membranes fractions were purified by Ficoll density gradient centrifugation as described before (35, 48, 61). Protein concentration was measured by the Bradford assay (63). ATP hydrolysis was measured by monitoring NADH oxidation spectrophotometrically (62) using 5 μg of total vacuolar membrane protein in the presence and absence of 100 nM concanamycin-A. Proton transport was measured by monitoring 9-amino-6-chloro-2-methoxyacridin quenching after addition of MgATP (48).

Author Contributions—K. J. P. conceived and coordinated the study, analyzed the results, and wrote the paper. C. Y. C. designed, performed, and analyzed the experiments. D. D. performed the PFK1 activity measurements.

Acknowledgments—We thank Dr. Jürgen Heinisch (Osnabrück) for generously providing the PFK-1 polyclonal antibodies. We thank Dr. Wayne Frasch for helpful discussions.

References

1. Forgac, M. (2007) Vacuolar ATPases: rotary proton pumps in physiology and pathophysiology. *Nat. Rev. Mol. Cell Biol.* **8,** 917–929
2. Kane, P. M. (2006) The where, when, and how of organelle acidification by the yeast vacuolar H^+-ATPase. *Microbiol. Mol. Biol. Rev.* **70,** 177–191
3. Parra, K. J., Chan, C. Y., and Chen, J. (2014) *Saccharomyces cerevisiae* vacuolar H^+-ATPase regulation by disassembly and reassembly: one structure and multiple signals. *Eukaryot. Cell* **13,** 706–714
4. Marshansky, V., Rubinstein, J. L., and Grüber, G. (2014) Eukaryotic V-ATPase: novel structural findings and functional insights. *Biochim. Biophys. Acta* **1837,** 857–879
5. Cotter, K., Stransky, L., McGuire, C., and Forgac, M. (2015) Recent insights into the structure, regulation, and function of the V-ATPases. *Trends Biochem. Sci.* **40,** 611–622
6. Breton, S., and Brown, D. (2013) Regulation of luminal acidification by the V-ATPase. *Physiology* **28,** 318–329
7. Hinton, A., Bond, S., and Forgac, M. (2009) V-ATPase functions in normal and disease processes. *Pflugers Arch.* **457,** 589–598
8. Muench, S. P., Trinick, J., and Harrison, M. A. (2011) Structural divergence of the rotary ATPases. *Q. Rev. Biophys.* **44,** 311–356
9. Zhao, J., Benlekbir, S., and Rubinstein, J. L. (2015) Electron cryomicroscopy observation of rotational states in a eukaryotic V-ATPase. *Nature* **521,** 241–245
10. Kane, P. M. (1995) Disassembly and reassembly of the yeast vacuolar H^+-ATPase *in vivo*. *J. Biol. Chem.* **270,** 17025–17032
11. Sumner, J. P., Dow, J. A., Earley, F. G., Klein, U., Jäger, D., and Wieczorek, H. (1995) Regulation of plasma membrane V-ATPase activity by dissociation of peripheral subunits. *J. Biol. Chem.* **270,** 5649–5653
12. Liberman, R., Bond, S., Shainheit, M. G., Stadecker, M. J., and Forgac, M. (2014) Regulated assembly of vacuolar ATPase is increased during cluster disruption-induced maturation of dendritic cells through a phosphatidylinositol 3-kinase/mTOR-dependent pathway. *J. Biol. Chem.* **289,** 1355–1363
13. Trombetta, E. S., Ebersold, M., Garrett, W., Pypaert, M., and Mellman, I. (2003) Activation of lysosomal function during dendritic cell maturation. *Science* **299,** 1400–1403
14. Dechant, R., Binda, M., Lee, S. S., Pelet, S., Winderickx, J., and Peter, M. (2010) Cytosolic pH is a second messenger for glucose and regulates the PKA pathway through V-ATPase. *EMBO J.* **29,** 2515–2526
15. Dechant, R., Saad, S., Ibáñez, A. J., and Peter, M. (2014) Cytosolic pH regulates cell growth through distinct GTPases, Arf1 and Gtr1, to promote Ras/PKA and TORC1 activity. *Mol. Cell* **55,** 409–421
16. Bond, S., and Forgac, M. (2008) The Ras/cAMP/protein kinase A pathway regulates glucose-dependent assembly of the vacuolar (H^+)-ATPase in yeast. *J. Biol. Chem.* **283,** 36513–36521
17. Oot, R. A., Huang, L. S., Berry, E. A., and Wilkens, S. (2012) Crystal structure of the yeast vacuolar ATPase heterotrimeric EGC(head) peripheral stalk complex. *Structure* **20,** 1881–1892
18. Tabke, K., Albertmelcher, A., Vitavska, O., Huss, M., Schmitz, H. P., and Wieczorek, H. (2014) Reversible disassembly of the yeast V-ATPase revisited under *in vivo* conditions. *Biochem. J.* **462,** 185–197
19. Kane, P. M. (2016) Proton transport and pH control in fungi. *Adv. Exp. Med. Biol.* **892,** 33–68
20. Martínez-Muñoz, G. A., and Kane, P. (2008) Vacuolar and plasma membrane proton pumps collaborate to achieve cytosolic pH homeostasis in yeast. *J. Biol. Chem.* **283,** 20309–20319
21. Parra, K. J., and Kane, P. M. (1998) Reversible association between the V1 and V0 domains of yeast vacuolar H^+-ATPase is an unconventional glucose-induced effect. *Mol. Cell. Biol.* **18,** 7064–7074
22. Lu, M., Ammar, D., Ives, H., Albrecht, F., and Gluck, S. L. (2007) Physical interaction between aldolase and vacuolar H^+-ATPase is essential for the assembly and activity of the proton pump. *J. Biol. Chem.* **282,** 24495–24503
23. Lu, M., Sautin, Y. Y., Holliday, L. S., and Gluck, S. L. (2004) The glycolytic enzyme aldolase mediates assembly, expression, and activity of vacuolar H^+-ATPase. *J. Biol. Chem.* **279,** 8732–8739
24. Chan, C. Y., and Parra, K. J. (2014) Yeast phosphofructokinase-1 subunit Pfk2p is necessary for pH homeostasis and glucose-dependent vacuolar ATPase reassembly. *J. Biol. Chem.* **289,** 19448–19457
25. Su, Y., Blake-Palmer, K. G., Sorrell, S., Javid, B., Bowers, K., Zhou, A., Chang, S. H., Qamar, S., and Karet, F. E. (2008) Human H^+ATPase a4 subunit mutations causing renal tubular acidosis reveal a role for interaction with phosphofructokinase-1. *Am. J. Physiol. Renal Physiol.* **295,** F950–F958
26. Banaszak, K., Mechin, I., Obmolova, G., Oldham, M., Chang, S. H., Ruiz, T., Radermacher, M., Kopperschläger, G., and Rypniewski, W. (2011) The crystal structures of eukaryotic phosphofructokinases from baker's yeast and rabbit skeletal muscle. *J. Mol. Biol.* **407,** 284–297
27. Heinisch, J. (1986) Construction and physiological characterization of mutants disrupted in the phosphofructokinase genes of *Saccharomyces cerevisiae*. *Curr. Genet.* **11,** 227–234
28. Arvanitidis, A., and Heinisch, J. J. (1994) Studies on the function of yeast phosphofructokinase subunits by *in vitro* mutagenesis. *J. Biol. Chem.* **269,** 8911–8918
29. Heinisch, J. (1986) Isolation and characterization of the two structural genes coding for phosphofructokinase in yeast. *Mol. Gen. Genet.* **202,** 75–82
30. Schrøder, T. D., Özalp, V. C., Lunding, A., Jernshøj, K. D., and Olsen, L. F. (2013) An experimental study of the regulation of glycolytic oscillations in yeast. *FEBS J.* **280,** 6033–6044
31. Brett, C. L., Tukaye, D. N., Mukherjee, S., and Rao, R. (2005) The yeast

endosomal Na^+K^+/H^+ exchanger Nhx1 regulates cellular pH to control vesicle trafficking. *Mol. Biol. Cell* **16,** 1396–1405
32. Ohya, Y., Umemoto, N., Tanida, I., Ohta, A., Iida, H., and Anraku, Y. (1991) Calcium-sensitive cls mutants of *Saccharomyces cerevisiae* showing a Pet- phenotype are ascribable to defects of vacuolar membrane H^+-ATPase activity. *J. Biol. Chem.* **266,** 13971–13977
33. Kane, P. M. (2007) The long physiological reach of the yeast vacuolar H^+-ATPase. *J. Bioenerg. Biomembr.* **39,** 415–421
34. Liu, J., and Kane, P. M. (1996) Mutational analysis of the catalytic subunit of the yeast vacuolar proton-translocating ATPase. *Biochemistry* **35,** 10938–10948
35. Owegi, M. A., Carenbauer, A. L., Wick, N. M., Brown, J. F., Terhune, K. L., Bilbo, S. A., Weaver, R. S., Shircliff, R., Newcomb, N., and Parra-Belky, K. J. (2005) Mutational analysis of the stator subunit E of the yeast V-ATPase. *J. Biol. Chem.* **280,** 18393–18402
36. Curtis, K. K., Francis, S. A., Oluwatosin, Y., and Kane, P. M. (2002) Mutational analysis of the subunit C (Vma5p) of the yeast vacuolar H^+-ATPase. *J. Biol. Chem.* **277,** 8979–8988
37. Smardon, A. M., and Kane, P. M. (2014) Loss of vacuolar H^+-ATPase activity in organelles signals ubiquitination and endocytosis of the yeast plasma membrane proton pump Pma1p. *J. Biol. Chem.* **289,** 32316–32326
38. Smets, B., Ghillebert, R., De Snijder, P., Binda, M., Swinnen, E., De Virgilio, C., and Winderickx, J. (2010) Life in the midst of scarcity: adaptations to nutrient availability in *Saccharomyces cerevisiae*. *Curr. Genet.* **56,** 1–32
39. Kresnowati, M. T., van Winden, W. A., Almering, M. J., ten Pierick, A., Ras, C., Knijnenburg, T. A., Daran-Lapujade, P., Pronk, J. T., Heijnen, J. J., and Daran, J. M. (2006) When transcriptome meets metabolome: fast cellular responses of yeast to sudden relief of glucose limitation. *Mol. Syst. Biol.* **2,** 49
40. Lenzen, S. (2014) A fresh view of glycolysis and glucokinase regulation: history and current status. *J. Biol. Chem.* **289,** 12189–12194
41. Ibáñez, A. J., Fagerer, S. R., Schmidt, A. M., Urban, P. L., Jefimovs, K., Geiger, P., Dechant, R., Heinemann, M., and Zenobi, R. (2013) Mass spectrometry-based metabolomics of single yeast cells. *Proc. Natl. Acad. Sci. U.S.A.* **110,** 8790–8794
42. Poulsen, A. K., Andersen, A. Z., Brasen, J. C., Scharff-Poulsen, A. M., and Olsen, L. F. (2008) Probing glycolytic and membrane potential oscillations in *Saccharomyces cerevisiae*. *Biochemistry* **47,** 7477–7484
43. Doherty, R. D., and Kane, P. M. (1993) Partial assembly of the yeast vacuolar H^+-ATPase in mutants lacking one subunit of the enzyme. *J. Biol. Chem.* **268,** 16845–16851
44. Nelson, N. (2003) A journey from mammals to yeast with vacuolar H^+-ATPase (V-ATPase). *J. Bioenerg. Biomembr.* **35,** 281–289
45. Shao, E., Nishi, T., Kawasaki-Nishi, S., and Forgac, M. (2003) Mutational analysis of the non-homologous region of subunit A of the yeast V-ATPase. *J. Biol. Chem.* **278,** 12985–12991
46. Arai, H., Pink, S., and Forgac, M. (1989) Interaction of anions and ATP with the coated vesicle proton pump. *Biochemistry* **28,** 3075–3082
47. Kawasaki-Nishi, S., Bowers, K., Nishi, T., Forgac, M., and Stevens, T. H. (2001) The amino-terminal domain of the vacuolar proton-translocating ATPase a subunit controls targeting and *in vivo* dissociation, and the carboxyl-terminal domain affects coupling of proton transport and ATP hydrolysis. *J. Biol. Chem.* **276,** 47411–47420
48. Chan, C. Y., Prudom, C., Raines, S. M., Charkhzarrin, S., Melman, S. D., De Haro, L. P., Allen, C., Lee, S. A., Sklar, L. A., and Parra, K. J. (2012) Inhibitors of V-ATPase proton transport reveal uncoupling functions of tether linking cytosolic and membrane domains of V0 subunit a (Vph1p). *J. Biol. Chem.* **287,** 10236–10250
49. Parra, K. J., Keenan, K. L., and Kane, P. M. (2000) The H subunit (Vma13p) of the yeast V-ATPase inhibits the ATPase activity of cytosolic V1 complexes. *J. Biol. Chem.* **275,** 21761–21767
50. Ho, M. N., Hirata, R., Umemoto, N., Ohya, Y., Takatsuki, A., Stevens, T. H., and Anraku, Y. (1993) VMA13 encodes a 54-kDa vacuolar H(+)-ATPase subunit required for activity but not assembly of the enzyme complex in *Saccharomyces cerevisiae*. *J. Biol. Chem.* **268,** 18286–18292
51. Diab, H., Ohira, M., Liu, M., Cobb, E., and Kane, P. M. (2009) Subunit interactions and requirements for inhibition of the yeast V1-ATPase. *J. Biol. Chem.* **284,** 13316–13325
52. Jefferies, K. C., and Forgac, M. (2008) Subunit H of the vacuolar (H^+) ATPase inhibits ATP hydrolysis by the free V1 domain by interaction with the rotary subunit F. *J. Biol. Chem.* **283,** 4512–4519
53. Parra, K. J., and Kane, P. M. (1996) Wild-type and mutant vacuolar membranes support pH-dependent reassembly of the yeast vacuolar H^+-ATPase *in vitro*. *J. Biol. Chem.* **271,** 19592–19598
54. Moore, K. J., and Fillingame, R. H. (2008) Structural interactions between transmembrane helices 4 and 5 of subunit a and the subunit c ring of *Escherichia coli* ATP synthase. *J. Biol. Chem.* **283,** 31726–31735
55. Rienmüller, F., Dreyer, I., Schönknecht, G., Schulz, A., Schumacher, K., Nagy, R., Martinoia, E., Marten, I., and Hedrich, R. (2012) Luminal and cytosolic pH feedback on proton pump activity and ATP affinity of V-type ATPase from *Arabidopsis*. *J. Biol. Chem.* **287,** 8986–8993
56. Müller, M. L., Jensen, M., and Taiz, L. (1999) The vacuolar H^+-ATPase of lemon fruits is regulated by variable H^+/ATP coupling and slip. *J. Biol. Chem.* **274,** 10706–10716
57. Kohio, H. P., and Adamson, A. L. (2013) Glycolytic control of vacuolar-type ATPase activity: a mechanism to regulate influenza viral infection. *Virology* **444,** 301–309
58. Fogarty, F. M., O'Keeffe, J., Zhadanov, A., Papkovsky, D., Ayllon, V., and O'Connor, R. (2014) HRG-1 enhances cancer cell invasive potential and couples glucose metabolism to cytosolic/extracellular pH gradient regulation by the vacuolar-H ATPase. *Oncogene* **33,** 4653–4663
59. Sennoune, S. R., and Martinez-Zaguilan, R. (2012) Vacuolar H(+)-ATPase signaling pathway in cancer. *Curr. Protein Pept. Sci.* **13,** 152–163
60. Ali, R., Brett, C. L., Mukherjee, S., and Rao, R. (2004) Inhibition of sodium/proton exchange by a Rab-GTPase-activating protein regulates endosomal traffic in yeast. *J. Biol. Chem.* **279,** 4498–4506
61. Ediger, B., Melman, S. D., Pappas, D. L., Jr., Finch, M., Applen, J., and Parra, K. J. (2009) The tether connecting cytosolic (N terminus) and membrane (C terminus) domains of yeast V-ATPase subunit a (Vph1) is required for assembly of V0 subunit d. *J. Biol. Chem.* **284,** 19522–19532
62. Lötscher, H. R., deJong, C., and Capaldi, R. A. (1984) Modification of the F0 portion of the H^+-translocating adenosinetriphosphatase complex of *Escherichia coli* by the water-soluble carbodiimide 1-ethyl-3-[3-(dimethylamino)propyl]carbodiimide and effect on the proton channeling function. *Biochemistry* **23,** 4128–4134
63. Bradford, M. M. (1976) A rapid and sensitive method for the quantitation of microgram quantities of protein utilizing the principle of protein-dye binding. *Anal. Biochem.* **72,** 248–254